UDC 539.4

# Calculation of the $\gamma$-TiAl Lattice Resistance

**R. C. Feng,[a,b] L. L. Li,[a,b] H. Y. Li,[a,b,1] Z. M. Wang,[a,b] and Z. X. Zhu[a,b]**

[a] Key Laboratory of Digital Manufacturing Technology and Application, The Ministry of Education, Lanzhou University of Technology, Lanzhou, China

[b] School of Mechanical and Electronical Engineering, Lanzhou University of Technology, Lanzhou, China

[1] cfrcly76@126.com

*The dislocation width and lattice resistance (Peierls stress) of a $\gamma$-TiAl alloy are calculated by the density ratio method. The lattice resistance is shown to decrease with the dislocation width. The relationship between the Peierls stress and dislocation width variation is defined by theoretical derivation. The yield stress is negatively correlated with the shear stress of the material. It can become a useful tool for choosing an appropriate shear stress under deformation.*

***Keywords***: $\gamma$-TiAl alloy, lattice resistance, dislocation, crystal interplanar spacing.

**Introduction**. The progress in aerospace and automotive industries require a higher level of comprehensive properties and lower weight materials compared to the currently used ones [1]. Because of its advantages, TiAl alloy has become a new type of high-temperature structure material with huge development potential and application prospects at high temperature [2, 3]. TiAl-based alloys have attracted wide attention [4]. However, as an intermetallic compound, low ductility and fracture toughness are its main weakness [5, 6]. So, it is very vital for improving the low temperature ductility to make these materials useful for industrial applications [7].

For high-temperature materials, the elastic modulus and yield strength are important mechanical properties of TiAl alloy [8]. The binary aluminum–titanium phase diagram is quoted in Fig. 1 [9] to show the intermetallic parts that we are focusing in this work. The plastic response of crystalline materials to an applied stress is determined by dislocation motion. Processes such as fatigue, dynamic recovery, and all stages of the plastic deformation curve (in particular, stage *III*) are controlled by the dynamic behavior of dislocation, including motion, cross-slip, multiplication and annihilation [10]. The stress–strain curve of single crystal material often has the form shown in Fig. 2. The curve in Fig. 2 consists of three phases: stages *I*, *II*, and *III*. Dislocation motion is a direct cause of crystal deformation. It can be activated only under certain stress conditions. There are many resistances need to be overcome in the process of the movement of dislocation. For example, precipitates, grain and twin boundaries [11]. The mobility of these defects largely determines the mechanical properties of the materials. Therefore, accurate prediction of lattice resistance for a dislocation is important to understand the mobility of the dislocation [12]. Zhang et al. [13] described the relationship between dislocation slip and fracture. But the relevant calculations is not given for the Peierls stress. In this paper, the width of dislocation and lattice resistance of $\gamma$-TiAl alloy is calculated, the facts indicate the lattice resistance decrease with the increase of the width of dislocation. In addition, the relationship between critical resolved shear stress and yield strength is obtained by the theoretical derivation.

1. **The Method of Calculation the Crystal Interplanar Spacing**. The method of density ratio is used to calculate the crystal interplanar spacing [14]. The areal density $\sigma$ is defined as the number of the total atoms of per unit area of crystal; the bulk density $\rho$ is

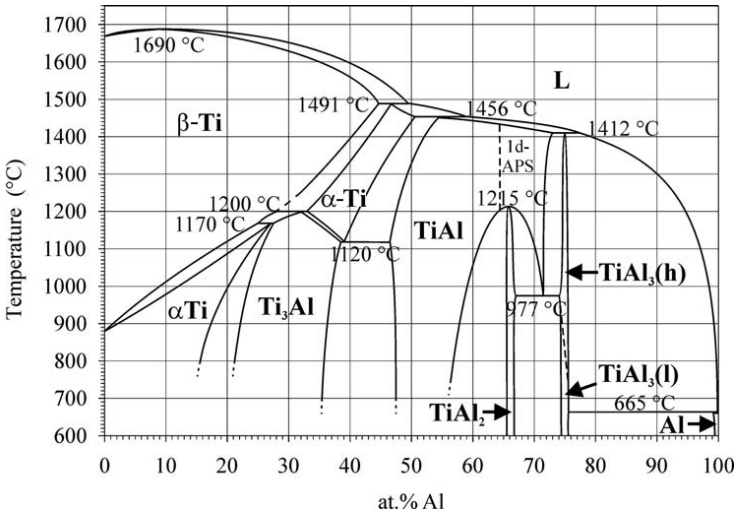


Fig. 1. The binary aluminum–titanium phase diagram.

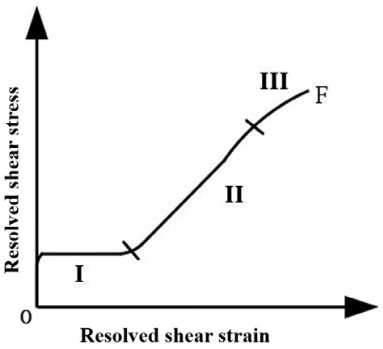


Fig. 2. Stress–strain curves of single crystal.

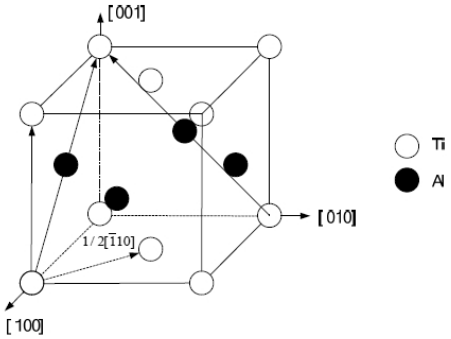


Fig. 3. The $L1_0$ structure of $\gamma$-TiAl.

defined as the number of the total atoms of a unit volume of crystal. Thus, the interplanar spacing of cubic lattices can be evaluated by

$$d_{hlk} = \frac{\sigma}{\rho}, \tag{1}$$

where $d_{hlk}$ is crystal interplannar spacing, $\sigma$ is areal density, and $\rho$ is bulk density.

2. **Calculation of the Crystal Interplanar Spacing with Face Centered Tetragonal (FCT) Structure**. The crystal structure of $\gamma$-TiAl alloy is shown in Fig. 3 [15]. According to Fig. 3 the volume of unit cell is *abc*, including four atoms. So the bulk density of lattice of $\gamma$-TiAl is expressed by formula (2)

$$\rho = \frac{4}{abc}. \tag{2}$$

The calculation of areal density is quite complex than volume density. The arrangement of atoms in different crystal interplanar is shown in Fig. 4. Taking an example for (100)

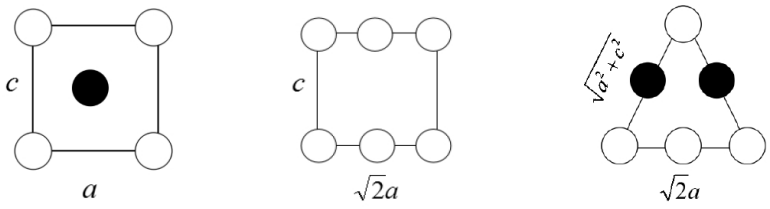


a b c

Fig. 4. The arrangement of atoms in different crystal interplanar: (a), (b), and (c) represent (100), (110), and (111) plane, respectively.

plane, which the area is *ac*. It contains two atoms. So the areal density can be represented by formula (3)

$$\sigma = \frac{2}{ac}. \tag{3}$$

As is known above, the crystal interplanar spacing of (100) plane can be written as

$$d_{(100)} = \frac{b}{2}. \tag{4}$$

Other crystal interplanar spacing can be obtained by referring to the above method. The results are listed in Table 1.

Table 1

**Crystal Interplanar Spacing of FCT Structure**

| Crystal face | Graphics area | Number of atoms | Areal density ($\sigma$) | Bulk density ($\rho$) | Interplanar spacing ($d$) |
|---|---|---|---|---|---|
| (100) | $ac$ | 2 | $2/ac$ | $4/abc$ | $b/2$ |
| (110) | $\sqrt{2}ac$ | 2 | $2/\sqrt{2}ac$ | $4/abc$ | $\sqrt{2}b/4$ |
| (111) | $\frac{\sqrt{2}a}{2}\sqrt{a^2/2+c^2}$ | 2 | $\frac{4}{\sqrt{2}a\sqrt{a^2/2+c^2}}$ | $4/abc$ | $\frac{bc}{\sqrt{2}\sqrt{a^2/2+c^2}}$ |

For the edge dislocation, the width of dislocation is $a/(1-\nu)$, where $a$ is crystal interplanar spacing and $\nu$ is Poisson's ratio. Through the above description, it is easy to obtain the width of dislocation in different slip plane. Therefore, the dislocation width are 2.6, 1.82, and 3.03(Å) in (100), (110), and (111) plane, respectively. However, the width of dislocation of screw dislocation is *a*. The width of dislocation on different slip planes is 2.0005, 1.41, and 2.24(Å), respectively. It is obvious that the width of dislocation on the (111) plane is the largest.

3. **Theoretical Calculations of Peierls–Nabarro Stress**. Peierls and Nabarro first estimated this fundamental quantity of the dislocation by using a continue model [16]. The Peierls stress is given as

$$\tau_{P-N} = \frac{2\pi}{b^2} E_{P-N} = \frac{2G}{(1-\nu)} \exp\left(-\frac{2\pi\omega}{b}\right), \tag{5}$$

Table 2

**The Physical Parameter of TiAl Alloy**

| Alloy | Shear modulus (GPa) | Elastic modulus (GPa) | Poisson's ratio | Reference |
|---|---|---|---|---|
| Ti–49.5Al | 70 | 176 | 0.23 | [17] |
| Ti–25.5Al | 56 | 144 | 0.28 | [18] |

where $G$ is shear modulus, $E$ is the Young modulus, $\nu$ is Poisson's ratio, $b$ is Burgers vector, and $\omega$ is the width of dislocation. Table 2 is the physical parameter of TiAl alloy.

From the classical dislocation theory, the most favorable slip systems should contain the close-packed lattice planes and the Burgers vectors with shortest shear displacements. Thus, dislocation slip in the $L1_0$ FCT structure favors the (111) planes along close or relatively close packed directions. According to the definition of the Burgers vector, the shortest lattice translation vectors which join two points in the lattice is choose as the Burgers vector. Substituting in Eq. (5)

$$\tau_{P-N} = \frac{2\times 70}{1-0.23}\exp\left(-\frac{2\pi\times 3.03}{2.8}\right). \tag{6}$$

The Peierls–Nabarro stress on (111) plane is 0.2041 GPa. It is the smallest lattice resistance in the TiAl alloy. It is because that the atomic spacing (Burgers vector) of close packed plane is least but crystal interplanar spacing (the width of dislocation) is largest. From the above calculations, it is clear that Peierls–Nabarro stress is low in TiAl alloy. In addition, the calculation of Peierls stress lead to an exponential dependence of $\tau_p$ on the dislocation width. Thus, the lattice resistance decrease with the increase of the dislocation width. The Peierls stress of other crystal interplanar is listed Table 3.

Table 3

**The Peierls Stress of Other Crystal Interplanar**

| Alloy | (100) (GPa) | (110) (GPa) | (111) (GPa) |
|---|---|---|---|
| Ti-49.5Al | 0.5329 | 3.0609 | 0.2041 |
| Ti-25.5Al | 0.3064 | 1.9104 | 0.1419 |

4. **Relationship between the Peierls Stress and Dislocation Strengthening**. Dislocation strengthening is a very important strengthening mechanism in metal. It can be caused by the increase in glide resistance that occurs when dislocations move, interact and change their distribution and density. The general form of dislocation strengthening is given by [19]:

$$\sigma = \sigma_0 + \alpha G b \rho^{1/2}, \tag{7}$$

where $\sigma_0$ is the Peierls stress, $G$ is shear modulus, $\rho$ is mobile dislocation density, $\alpha$ is a constant equaling about 0.3, and $b$ is Burgers vector. The Peierls stress is a constant and the value is relatively small in TiAl alloy. So the dislocation density play mainly role for the dislocation strengthening. When considering hardening, the strain rate, dislocation density and dislocation rate have a relationship as following [19]:

$$\dot{\varepsilon} = mb\rho v. \tag{8}$$

Substituting into Eq. (7)

$$\sigma = \sigma_0 + \alpha G b \left( \frac{\dot{\varepsilon}}{mbv} \right)^{1/2}, \tag{9}$$

where $v$ is dislocation rate and $m$ is Schmid factor.

Studies on face-centered cubic (FCC) and hexagonal close-packed (HCP) crystals have shown that at the critical resolved shear stress (CRSS) for macroscopic slip satisfies [16]

$$v = A\tau^n. \tag{10}$$

Thus, the Eq. (9) can become

$$\sigma = \sigma_0 + \alpha G b \left( \frac{\dot{\varepsilon}}{mbA\tau^n} \right)^{1/2}, \tag{11}$$

where $A$ is a material constant and $n$ is a constant.

During the tensile deformation, the strain rate can be treated as a fixed value. Therefore, only when the CRSS is the smallest, the effect of strengthening is most obvious. In polycrystal, the relationship between the yield stress and the dislocation is the same as that observed for single crystal [18]. But the individual grains usually have a random orientation with respect to one another. So grain boundaries have a very important role in the deformation of polycrystalline materials. From experiment measurement of the yield stress of poly aggregates in which grain size $d$ is the only material variable, it has been found that Hall–Petch relationship is satisfied [19]:

$$\sigma_y = \sigma_0 + kD^{1/2}. \tag{12}$$

where $\sigma_y$ is the yield stress, $\sigma_0$ is a frictional stress required to move dislocation, $k$ is the Hall–Petch slope, and $D$ is the grain size. This indicates that the mechanical properties of TiAl alloy can be improved by the refinement of grain size.

5. **Results and Discussion**. The Peierls stress arises as a direct consequence of the periodic structure of the crystal lattice and depends sensitively on the form of the force–distance relation among individual atoms. But the dependence of $\tau_p$ on temperature is complex. Dietze [20] took account of thermal vibrations by smearing the sampling points with a Gaussian distribution corresponding to the thermal vibrational motion. As a result, if the dislocation is $\omega(T)$ Burgers vector wide at a temperature of $T$ [$\omega(T) = 2\xi/b$], it is related to its width at 0 K, $\omega_0$, by [21]

$$\omega(T) = \omega(0)\exp(T/3T_m), \tag{13}$$

where $T_m$ is the melting point and $\xi$ is half-width of the dislocation.

Substituting this relationship into Eq. (5), one obtains the $\tau_p$ at temperatures above the Debye temperature, $\tau_p(T)$,

$$\frac{\tau_p}{G} = \left\{ \frac{1}{1-\nu} \right\}^{-T/3T_m} \left\{ \frac{\tau_p}{G} \right\}^{\exp(T/3T_m)}, \tag{14}$$

where $G$ is shear modulus at 0 K.

Equation (14) can be used to probe the temperature dependence of $\tau_p$.

**Conclusions**. To summarize, the crystal interplanar spacing of $\gamma$-TiAl alloy is obtained by the method of density ratio in this paper. Besides, the width of dislocation and lattice resistance of $\gamma$-TiAl with a $L1_0$-type ordered structure is calculated. The calculation shows that there is a clear correlation between $\tau_p$ and $\omega/b$ for the $\gamma$-TiAl alloy. This is consistent with the characteristics of other metal. Through the calculation of the Peierls stress of $\gamma$-TiAl. It can provide an effective evidence for the movement of dislocation and the activation of the slip system. In addition, the relationship of critical resolved shear stress and yield stress is obtained by the theoretical derivation. It indicates that only when the critical resolved shear stress is the smallest, the reinforcement is most obvious.

***Acknowledgments***. This work was supported by a grant from the National Science Fundation of China (No. 51665030) and the Program for ChangJiang Scholars and Innovative Research Team in University of Ministry of Education of China (No. IRT_15R30) and Doctoral research Foundation of Lanzhou University of Technology. The authors wish to thank Engineering Research center of Nonferrous Metallurgy's New Equipment, Ministry of Education, Lanzhou University of technology for providing help.

1. Z. Wu, R. Hu, T. Zhang, et al., "Microstructure determined fracture behavior of a high Nb containing TiAl alloy," *Mater. Sci. Eng. A*, **666**, 297–304 (2016).
2. H. Clemens and S. Mayer, "Design, processing, microstructure, properties, and applications of advanced intermetallic TiAl alloys," *Adv. Eng. Mater.*, **15**, No. 4, 191–215 (2013).
3. R. C. Feng, Z. Y. Rui, G. T. Zhang, "Improved method of fatigue life assessment for TiAl alloys," *Strength Mater.*, **46**, No. 2, 183–189 (2014).
4. M. Terner, S. Biamino, D. Ugues, et al., "Phase transitions assessment on $\gamma$-TiAl by Thermo Mechanical Analysis," *Intermetallics*, **37**, 7–10 (2013).
5. Y. Ma, D. Cuiuri, N. Hoye, et al. "The effect of location on the microstructure and mechanical properties of titanium aluminides produced by additive layer manufacturing using in-situ alloying and gas tungsten arc welding," *Mater. Sci. Eng. A*, **631**, 230–240 (2015).
6. S. Tian, X. Lv, H. Yu, et al.,"Creep behavior and deformation feature of TiAl–Nb alloy with various states at high temperature," *Mater. Sci. Eng. A*, **651**, 490–498 (2016).
7. M. Kanani, A. Hartmaier, and R. Janisch, "Stacking fault based analysis of shear mechanisms at interfaces in lamellar TiAl alloys," *Acta Mater.*, **106**, 208–218 (2016).
8. J. L. Su and X. F. Lian, "Relationship between intrinsic characteristic sizes of elastic property and plastic property of $\gamma$-TiAl based alloy," *Chinese J. Nonferr. Metal.*, **25**, No. 2, 338–343 (2015).
9. J. C. Schuster and M. Palm, "Reassessment of the binary Aluminum-Titanium phase diagram," *J. Phase Equilib. Diff.*, **27**, No. 3, 255–277 (2006).
10. E. Oren, E. Yahel, and G. Makov, "Dislocation kinematics: a molecular dynamics study in Cu," *Model. Simul. Mater. Sc.*, **25**, No. 2, 025002 (2017).
11. Z. Li, N. Mathew, and R. C. Picu, "Dependence of Peierls stress on lattice strains in silicon," *Comp. Mater. Sci.*, **77**, 343–347 (2013).
12. G. Liu, X. Cheng, J. Wang, et al., "Improvement of nonlocal Peierls–Nabarro models," *Comp. Mater. Sci.*, **131**, 69–77 (2017).
13. G. T. Zhang, Z. Y. Rui, R. C. Feng, et al., "Illustration of fracture mechanism in high temperature for TiAl alloys," *Appl. Mech. Mater.*, **457–458**, 19–22 (2014).

14. L. Wang, "Calculation of the interplanar spacing of cubic crystal lattice," *J. Yunnan Nat. Univ.*, **24**, No. 4, 346–348 (2015).
15. R. C. Feng, J. T. Lu, H. Y. Li, et al., "Effect of the microcrack inclination angle on crack propagation behavior of TiAl alloy," *Strength Mater*., **49**, No. 1, 75–82 (2017).
16. D. Hull and D. J. Bacon, *Introduction to Dislocations*, Butterworth-Heinemann (2011).
17. R. E. Schafrik, "Dynamic elastic moduli of the titanium aluminides," *Metall. Trans. A*, **8**, No. 6, 1003–1006 (1977).
18. K. Tanaka, K. Okamoto, H. Inui, et al., "Elastic constants and their temperature dependence for the intermetallic compound $Ti_3Al$," *Philos. Mag. A*, **73**, No. 5, 1475–1488 (1996).
19. D. François, A. Pineau, and A. Zaoui, *Mechanical Behaviour of Materials*, Springer, Dordrecht (1998).
20. H.-D. Dietze, "Die Temperaturabhängigkeit der Versetzungsstruktur," *Z. Phys.*, **132**, No. 1, 107–110 (1952).
21. J. N. Wang, "Prediction of Peierls stresses for different crystals," *Mater. Sci. Eng. A*, **206**, No. 2, 259–269 (1996).

Received 15. 03. 2018